BROAD-BAND 3-D PHYSICS-BASED SIMULATION OF EARTHQUAKE-INDUCED WAVE-FIELD AT THE KASHIWAZAKI-KARIWA NUCLEAR POWER PLANT (JAPAN): AN ALL-EMBRACING SOURCE-TO-SITE APPROACH.

F.GATTI[1], S.TOUHAMI[1], F.LOPEZ-CABALLERO[1], D.CLOUTEAU[1], V. ALVES FERNANDES[2], M.KHAM[2]

[1]Laboratoire MSSMat UMR CNRS 8579-CentraleSupélec

[2]Electricité de France-R&D

E-mail contact of main author: filippo.gatti@centralesupelec.fr

Abstract. The influence of the regional 3-D geology on the synthetic earthquake ground motion prediction is herein assessed, studying the seismic response of Kashiwazaki-Kariwa nuclear power plant (KKNPP), during the 2007 Niigata seismic sequence (west Japan), so to explore the potentiality and practicability of the innovative computational tools available. This applicative case study was chosen within the framework of the SINAPS@ project, the first French research project which aims to propose a continuous approach from the fault to the structure and equipment's, accounting explicitly for the uncertainties related to the databases and the models. A source-to-site numerical model of the region (≈ 60 km wide) is built-up and calibrated for small aftershocks including surface topography, Japan sea and complex 3-D underground foldings. The impact of complex 3-D geology in terms of seismic response at KKNPP is quantified, by comparison with the simplified transverse isotropic geology. This validation stresses the importance of the 3-D geology and explicates the observed high ground motion spatial variability, as well as the strong dependence of the site response on the incident wave obliquity. The synthetic wave-field (0-5 Hz) is obtained by employing SEM3D, a high-scalable software tailored based on the Spectral Element Method. This high-fidelity code performs efficiently (thanks to its high scalability on parallel supercomputers) when refining the model spatial discretization and increasing the bedrock-to-sediment shear wave velocity gradient. The synthetic wave-motion simulated was exploited as input motion for a Soil-Structure Interaction numerical model (Finite Element Method - Boundary Element Method, Code_Aster-MISS3D) of the standard reactor building at KKNPP. The impact of the 3-D geology is assessed therefore on the structural components, highlighting a considerable amplification compared to the case of layered one.

Key Words: broad-band, source-to-structure, KKNPP, SEM3D, code_aster.

1. INTRODUCTION

In this paper, the latest achievements in the construction of 3-D Broad-Band Source-to-Structure (BBS2S) earthquake scenario are presented, in terms of forward numerical analysis of a complex applicative case. This study stems from the French national research program SINAPS@ (https://www.institut-seism.fr/projets/sinaps/) [1], whose main goal is to re-evaluate the current seismic design standards of nuclear facilities on French territory. The manifold overall goal of this ongoing research project is to review the traditional and current experimental and numerical approaches to study an earthquake and to design the structural response to a ground shaking by employing a rigorous uncertainty quantification routine at each modeling stage and to all the input parameters and related databases.

In the past two decades, the seismic hazard analysis and vulnerability assessment of large

urban areas and strategical structures and infrastructures have progressively taken advantage of the impressive achievements in High-Performance Computing (HPC). This outstanding technological and numerical progress paves the way and steer the leap towards a full coupling between the large scale seismological models for the region of interest (i.e. the fault mechanism and the geological properties of the Earth's crust, the presence of surface/buried topography and bathymetry) with local engineering models for geotechnical, site-effect and structural analyses. This holistic all-embracing approach is backed by the constant development of highly portable multi-tool computational platforms, capable of handling the manifold nature of the multi-scale/-dimension earthquake phenomenon, as well as to produce several realizations of the same scenario, within the framework of seismic risk evaluation [5, 17,22,24].

In spite of the inherent complexity and the huge dimensions of those computational models, their power is essentially embodied by the higher broad-band accuracy they provide (i.e. up to 4-5 Hz) [2,3], gradually bridging the gap between low-frequency source models obtained via wave-form inversion techniques and the structural modal frequencies (i.e. up to 20 Hz). This trend is expected to increase in the very near future, owing the seemingly unstoppable growth of the HPC resources (towards exascale engineering simulations) [4]. In the meanwhile, and alternatively, broad-band synthetic ground motion prediction can be obtained by hybrid modeling. Starting from an idea of Graves and Pitarka [5], the long-period (LP) part of the simulated ground motion is sealed at each station with stochastic or empirical predictions at high frequencies, to cope with the intrinsic poor accuracy of numerical physics-based analysis methods. Alternatively, the LP simulated synthetic wave-field are employed to simulate the short period (SP) part of the synthetic wave-forms.

In this context, this study presents the outcome of a numerical exercise performed on a real source-to-structure earthquake scenario, that can be unraveled into the following three issues:

1. The resolution of the source-to-site wave-propagation problem by high-fidelity 3-D numerical model of the region of interest, in a 0-7 Hz frequency range (see section 2).
2. The high-frequency enrichment of the obtained synthetic time-histories (up to 30 Hz) by scaling their pseudo-acceleration spectra onto the SP prediction provided by trained Artificial Neural Networks (see section 3).
3. The analysis of the structural response of one nuclear reactor building in a Soil-Structure Interaction (SSI) framework, by injecting the enriched synthetic wave motion in a 3-D Finite Element Method (FEM) model of the structural components, exploiting a Boundary Element Method (BEM) to compute the impedance functions (see section 4).

Specifically, the analysis targets the numerical prediction of the seismic response of the Japanese nuclear site of Kashiwazaki-Kariwa (KKNPP), held by the Tokyo Electric Power Company (TEPCO). In 2007, the Mw6.6 Niigata-Ken Chūetsu-Oki earthquake (NCOEQ-2007, FIG. 1a) struck KKNPP, although no major disasters occurred. The NCOEQ-2007 affected an area of approximately 100 km of radius along the coastal line of South-West Niigata prefecture, till a maximum depth of 17 km [6]. The plant consists of 7 generators (see map in FIG. 1b) and it is located on the hanging wall of the seismogenetic fault that triggered the NCOEQ-2007 event. The strong motion sensors indicated that during the main shock the site experienced nearly twice the Peak Ground Acceleration (PGA) considered in the plant design. Moreover, the rather high variability of PGA values within the site area is representative of directivity features of the source radiation (see [7] for an extensive review of the observed recordings and site-effect reconnaissance, as well as the results of the benchmark

organized under the auspices of the International Atomic Energy Agency (IAEA), of the Nuclear Energy Agency (NEA) is a specialised agency within the Organisation for Economic Co-operation and Development (OECD), IAEA-TECDOC-1722 [28]).

The analysis presented hereafter is intended to clarify some aspects of the recorded site-effects in the epicentral area (within the japanese Niigata prefecture) and at the KKNPP, mainly concerning the assessment of the influence of the deep geological complex structure on the KKNPP site response, compared to traditional sub-horizontally layered model. Shallow small earthquake sources are considered (belonging to the 2007 NCOEQ aftershock cluster) so to discount the rupture directivity effect and focus on the near-field wave motion generated by the interaction with the geological interfaces.

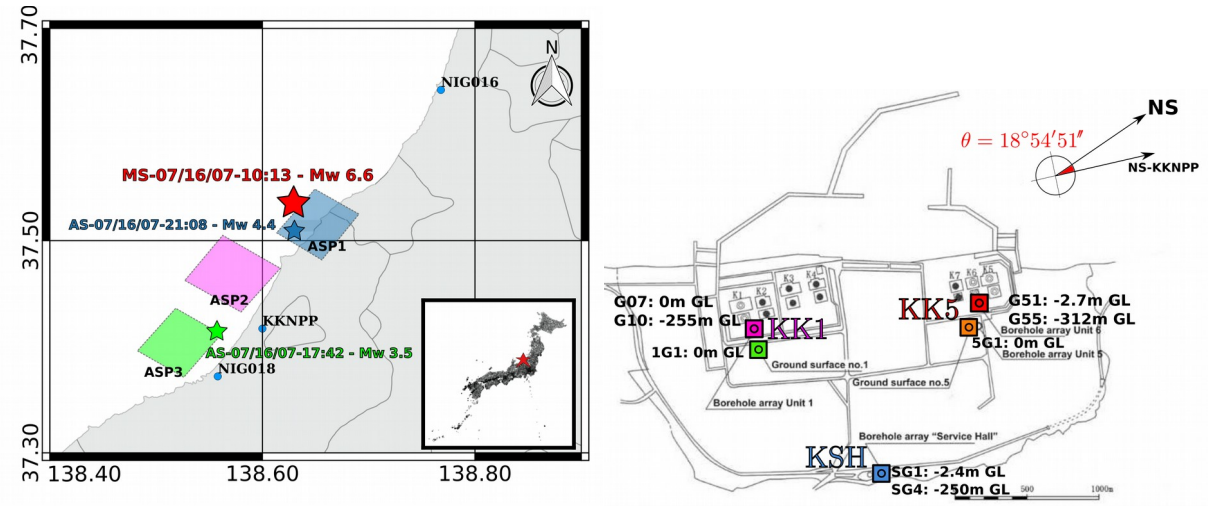

(a) (b)

FIG. 1. (a) Map of the KKNPP with the accelerometric stations installed that recorded the NCOEQ. (b) Map of the Niigata area surrounding the 2007 NCOEQ epicentre. The three major fault asperities are indicated by the colored rectangles.

2. HIGH-FIDELITY PREDICTION OF THE REGIONAL WAVE FIELD

2.1 Data and Methods

Several authors [8,9,10] showed that the large amplitude of Unit 1 (located on the southwestward part of the KKNPP) comes from the folding structure underlying the Niigata region. The latter has been proven to be rather intricate. Several 1-D and 3-D models of the velocity structure have been proposed in the past, based on geological and geophysical explorations [11]. Despite the good approximation of the regional incident wave motion obtained with simplified 1-D and 3-D geological configurations in the surroundings of the epicentral area, there is consensus among many researchers [8,9,12,13] that none of them is suitable to picture the spatial variability of the ground motion observed at KKNPP. With this regard, [9,13] related this observation to the presence of a folded structure underneath KKNPP (characterized via boring and seismic reflection surveys [14]), which composes of the Madonosaka syncline, located between the Ushirodani and Chuo-Yutai anticlines [15]. The folding cross-section extends for approximately 7 km across the Japanese coastline, up to 2.5 km down depth and with its hinge axes (i.e. the directrixes) strike at N55°E, as shown in FIG. 2a. Unit 1 is located on the synclinal axis.

The geographical distribution of this peculiar sediment conformation shears through the nuclear facility, with the Ushirodani anticline and Madonosaka syncline placed below Unit 5 and Unit 1 respectively. The Chuo-Yatai anticline is indicated as well, which seemingly passes in the Service Hall surroundings (array KSH).

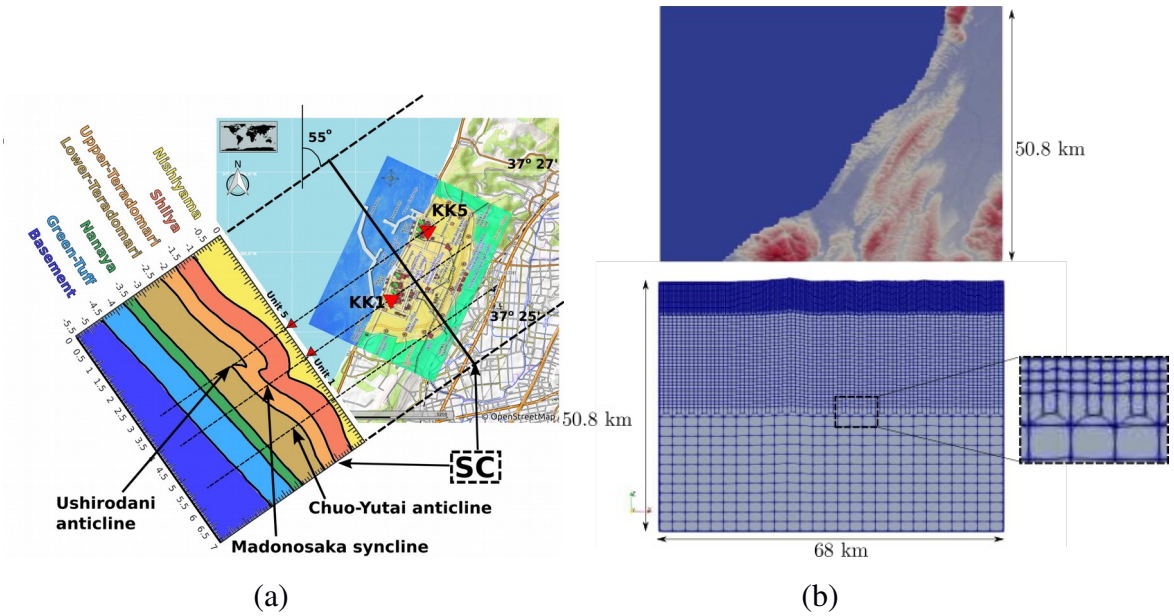

FIG. 2. (a) Schematic structural map of the series of Ushirodani anticline - Madonosaka syncline, located underneath KKNPP. (b) Detail of the SEM3D mesh, including topography and bathymetry, constructed for the test case herein.

The latter 3-D geology is defined by seven strata (see FIG. 2a, corresponding to section S4 in [10]). Table 1 shows the main features of the mentioned structure, obtained by geophysical surveys.

TABLE 1. GEOLOGICAL PROPERTIES OF THE FOLDING STRUCTURE UNDERNEATH KKNPP. Vp AND Vs ARE THE PRESSURE- AND SHEAR-WAVE VELOCITIES RESPECTIVELY. THE ** INDICATES THE INTERFACE CHOSEN TO PLUG THE FOLDING STRUCTURE INTO THE ORIGINAL 1-D AOCHI2013 PROFILE, GRANTING A SMOOTH TRANSITION FROM ONE MODEL TO THE OTHER.

Layer	**Vs [m/s]**	**Vp [m/s]**	**Density [kg/m^3]**
Nishiyama	700	1900	1700
Shiiya	1200	2200	2100
Upper Teradomari	1700	3300	2300
Lower Teradomari	2000	4200	2400
Nanatani	2000	4600	2500
**Green Tuff	2600	5200	2600
Seismic bedrock	2600->5200	5200	2600

Given the complex geological structure (see [8] and [10] for further details), and with the twofold aim to reproduce the overall regional wave-field, yet focusing on a realistic broad-band simulation of the incident ground motion in the KKNPP surroundings, a hybrid geological model of the Niigata region was herein constructed in two steps, progressively adding all the available information. First of all, the layered profile proposed by [16] (hereafter referred as Aochi2013, see Table 2) was selected as representative for the propagation of the long period ground motion (i.e. 0.1-3.75 Hz) at a regional scale (i.e. approximately 90km × 83 km × 82 km).

TABLE 2. PROPERTIES OF THE AOCHI2013 PROFILE (AOCHI ET AL. 2013). Z REPRESENTS THE DEPTH OF THE UPPER LAYER SURFACE, VP AND VS ARE THE P-WAVE AND S-WAVE VELOCITIES RESPECTIVELY, Qp AND Qs THE QUALITY FACTORS FOR P-WAVE AND S-WAVE RESPECTIVELY. THE * INDICATES THE INTERFACE CHOSEN TO PLUG THE FOLDING STRUCTURE INTO THE 1-D AOCHI2013 PROFILE, GRANTING A SMOOTH TRANSITION FROM ONE MODEL TO THE OTHER.

Z [km]	Vp [km/s]	Qp [1]	Vs [km/s]	Qs [1]
0.0	2.28	200.0	1.02	100.0
0.5	2.57	228.7	1.23	100.0
1.0	2.93	257.1	1.51	100.0
1.5	3.09	293.3	1.63	100.0
2.0	3.25	309.1	2.09	100.0
3.0	3.68	325.9	2.33	100.0
4.0	4.03	368.2	2.49	100.0
*5.0	4.30	403.2	2.75	100.0
6.0	4.55	430.9	2.89	100.0

From now on, it will be referred as to the LARGE model. Its considerable extension was mainly chose to grant a minimal coverage of the NW regional wave-field. Thus LARGE model was designed so to include part of the Sado Island in front of the Niigata region, where the K-NET station NIG004 is located. The Japan sea presence was disregarded at this step, along with related bathymetry and coastline. The LARGE model was then trimmed and adjusted so to plug the 3-D Ushirodani anticline - Madonosaka syncline - Chuo-Yatai anticline structure into it, following the previous work of [10] (see FIG. 2b). The 1-D profile, issued from Aochi2013, was welded to the syncline-anticline system by adjusting and linearly smoothing the uppermost crustal material discontinuities to reconnect with the external layered geology of LARGE model. This choice was justified to avoid the possible spurious noise generated by the interaction of the incident wave-field with some fictitious geological discontinuities between the folding domain and the outer domain, which would pollute the synthetics. With respect to the LARGE model, the SMALL one, featured by a minimal shear-wave velocity of 700 m/s was designed to accurately propagate up to 5.0 Hz, considering a third order Lagrange polynomial degree. In the SMALL model, moreover, the Japan sea was considered.

For the sake of brevity, the calibration of the LARGE model, in a lower-frequency range, is herein omitted. Further details, refer to [17]. However, in the next section, the comparison between recordings and simulations (SMALL model) are provided, both considering the mentioned folded geological model (FLD) and its sub-horizontally layered counterpart,

obtained by simply smoothing the folding surfaces to plane interfaces and reconnecting them with the external Aochi2013 model.

The simulation of realistic source-to-site ground shaking scenarios requires a reliable estimation of several different parameters, related to the source mechanism, to the geological configuration and to the mechanical property of the soil layers and crustal rocks. Due to the enormous extension of those regional scale scenarios, the degree of uncertainty associated to the whole earthquake process (from fault to site) is extremely high. Another drawback resides on the computational effort required to routinely solve the wave propagation on such huge domains and over such a great number of DOFs (Degrees of Freedom). At this point, it appears necessary to build up a multi-tool virtual laboratory to construct and calibrate the seismological model. To this end, three main issues must be tackled:

1. to mesh the domain of interest, its geological conformation (bedrock to sediment geological surfaces), the surface topography and the bathymetry (if present)
2. to represent the material rheology (i.e., elastic, viscous-elastic, non-linear hysteretic)
3. to describe the natural heterogeneity of the Earth's crust and soil properties, at different scales (i.e., regional geology, local basin-type structures and heterogeneity of granular materials)

Among the tools employed hereafter, the main wave propagation solver is herein represented by a software called SEM3D, tailored to efficiently solve the wave propagation problem, by means of the Spectral Element Method (SEM). SEM3D has been developed based upon the RegSEM code [18,19]. The SEM is a high-order version of the Finite Element Method and it has recently become predominant due to its accuracy and straight-forward extension to parallel implementation, and it is well known to provide an accurate solution of the elasto-dynamic problem in highly heterogeneous media [20]. The original core of the SEM3D software allowed to solve the wave propagation problem in any velocity model, including anisotropy, intrinsic attenuation and Newtonian fluid-structure interaction. Moreover, the code makes use of a library called HexMesh (https://github.com/jcamata/HexMesh.git), that implements an efficient linear 27-tree finite element mesh generation scheme [21] and it is capable to generate large computational grids (i.e. ≈ 100 km) by extruding the Digital Elevation Model (DEM) provided and progressively top-down coarsen it, so to obtain a non-structured grid. HexMesh easily handles coastlines and bathymetries, by cutting and locally refining the generated grid accordingly.
The geological interfaces were introduced by a *not honouring* approach, which means the transition between geological domains is obtained by linearly interpolating the spatially distributed mechanical properties on the integration points used for the spectral approximation.

2.2 Results and discussion

Due to the asymmetric nature of the folded structural geology beneath the KKNPP site, two small aftershocks (see Table 3) scenarios were simulated (f_{max}=5 Hz), whose hypocenters were located along the directrix of the Madonosaka syncline, at the two opposite sides with respect to its planar cross-section passing through the TEPCO facility (FIG. 3a). The after-shocks were simulated as double-couple seismic moment, with respective rise times τ_R indicated in Table 3.

TABLE 3. FOCAL MECHANISMS OF THE TWO AFTERSHOCKS INVESTIGATED IN THIS PAPER, BELONGING TO THE NCOEQ2007 SEISMIC SEQUENCE.

	dd/mm/yy-hh:mm	Mw	Strike [°]	Slip [°]	Dip [°]	T_R [s]
AS1	07/16/07-21:08	4.4	187	70	54	0.113
AS2	07/16/07-17:42	4.2	309	78	37	0.045

The aim is to characterize the 3-D effect of such a complex geology, by spanning different incidence angles of the wave-front impinging the KKNPP. Except the eventual poor reproduction of the late surface wave arrivals, general features of observed records for AS1 and AS2 could be reproduced, as portrayed in FIG. 3b-3e for AS1 (with the northernmost epicenter, although similar results were obtained for AS2, with the southernmost one). The improvement granted by the inclusion of the folded configuration however is evident (red traces in FIG.s 3b-3e), compared to the poor fit to the records obtained with a sub-horizontally layered geology not including the folding (green traces). Finally, the KKNPP site response estimated by SEM3-D analyses for AS1 and AS2 is condensed in the following figures that portray the pseudo-spectral acceleration spectra Sa estimated at KKNPP, for AS1 (FIG. 4a) and AS2 (FIG. 4b) respectively. Hayakawa et al. [22] showed that the large amplitude of Unit 1 (located on the southwestward part of the KKNPP) comes from the folding structure where Unit 1 is located on the synclinal axis (FIG. 4a).

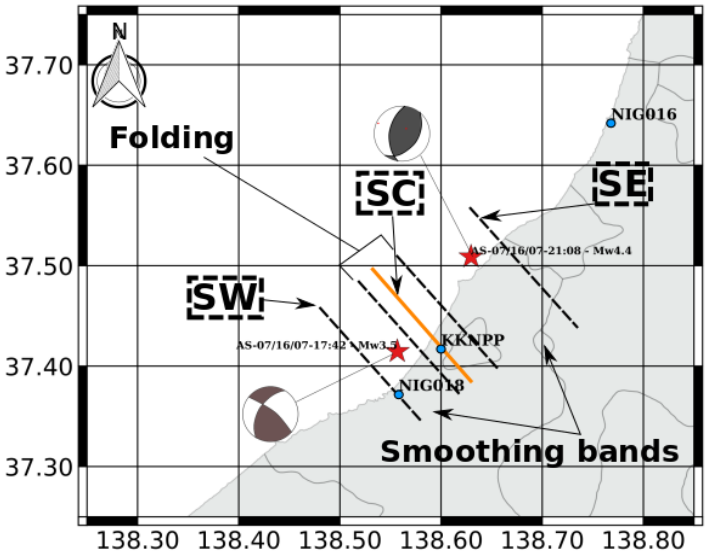

(a)

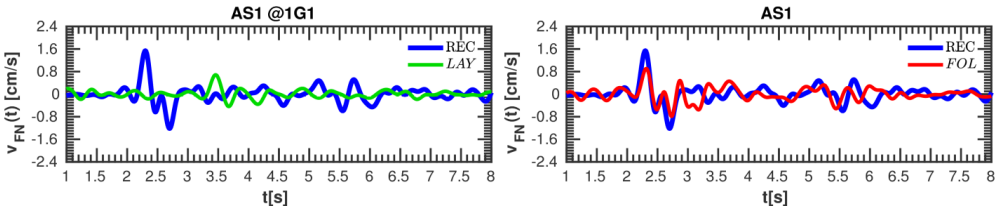

(b) (c)

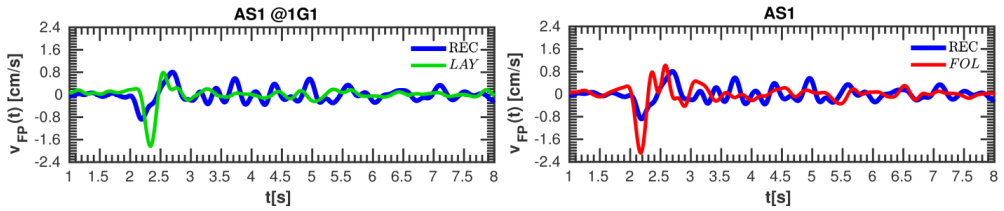

(d) (e)

FIG 3. (a) Geographical map of the KKNPP surroundings, depicting folded cross-section SC, the smoothing bands and the extrusion edged, cross-sections SE and SW. The two aftershocks indicated by red stars are referred as AS1, located northwest of KKNPP and AS2, located southeast of KKNPP. (b-c) Comparisons between recordings (REC, blue) and simulation with layered geology (LAY, green) and folded geology (FOl, red) respectively on the fault-normal direction, for AS1. (d-e) Same as (b-c) for fault-parallel direction. All the time-histories were band-pass filtered between 0.15-5.0 Hz.

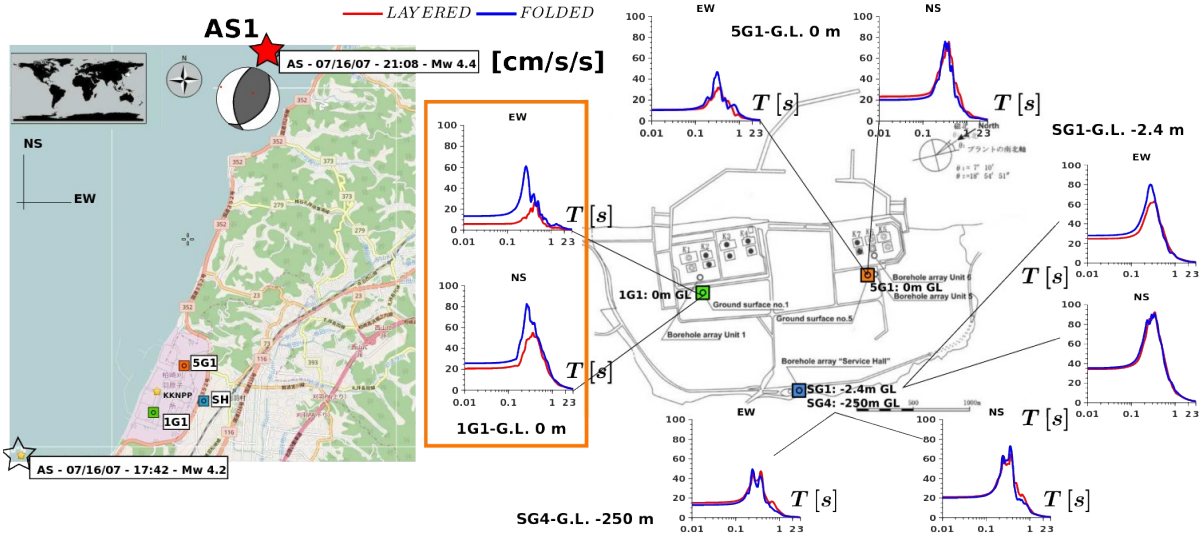

(a)

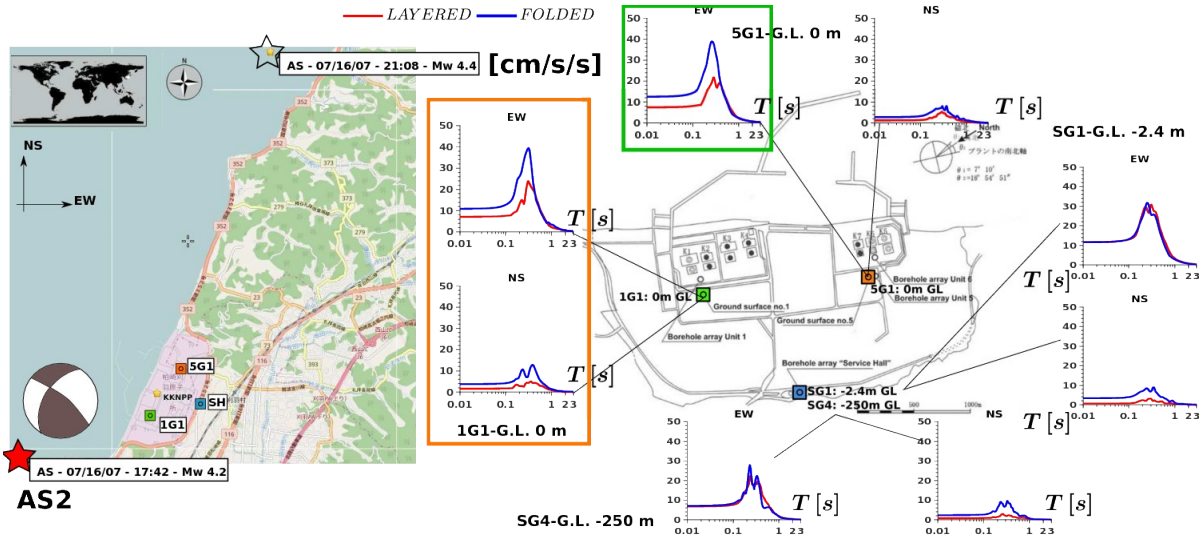

(b)

FIG 4. (a) AS1: Sa response spectra (in cm/s2) at different location around the KKNPP site. LAY-ERED (red) and FOLDED geological models were compared. (b) AS2: Sa response spectra (in

cm/s2) at different location around the KKNPP site. LAYERED (red) and FOLDED geological models were compared. All the time-histories were band-pass filtered between 0.15-5.0 Hz.

In agreement with what proposed in the literature, FIG.s 4a-4b indicate the folded geology as responsible of higher peaks for the response spectra obtained nearby Unit 1, for natural periods T < 0.5s . The site response at Unit 5 and Service Hall is seemingly unaltered by the introduction of a complex folding structure beneath KKNPP. The minimum shear velocity introduced in the model corresponds to the engineering bedrock related to depth, justifying that the spatial incoherence of the ground motion recorded at surface and specifically the amplification southwestward are extremely influenced by the syncline-anticline structure, despite the effects due to shallow borehole geology (dispersion, attenuation/amplification) which have been disregarded in the analysis. This strengthens the argument that the site response at the Service Hall (which is located above Chuo-Yutai anticline) depended mainly on the non-linear site-effects taking place at shallow depths (i.e. G.L.-250 m). The amplification trend occurs independently on the source position, being more accentuated along the EW direction. [8] showed that the Upper Teradomari stratum does not alter the wave-propagation of up-going waves, which tend to focalize at the Madonosaka syncline passing through Shiiya stratum. Site amplification becomes therefore significant at Unit 1. On the other hand, Unit 5 (which is located above the Ushirodani anticline) is evidently more sensitive to wave-motion travelling from South-West to North-East, throughout the folding zone: the pseudo-spectral peaks differs from layered to folded geology only in FIG. 4b, referring to AS2 (nucleated close by the third asperity on the fault rupture plane). It is worth mentioning that the described geological model has a minimum shear-wave of 700 m/s, which represents the *engineerin bedrock* appearing found downhole at depths below 150-250 m by TEPCO site characterization. The uppermost soil layers (Nishiyama, Yasuda, Banjin strata) are softer layers, which underwent major non-linear shearing effects during the NCOEQ2007 main shock. The mesh designed herein was not able to render such a finer geological description, concurring at the discrepancies between the recordings and the synthetics.

3. Applying ANN2BB to synthetic ground motion

3.1 Design and Training of Artificial Neural Networks for spectral acceleration prediction

The earthquake ground motion simulations performed in [17] are reliable to 5 Hz. Although outstanding, this twofold modeling and computational endeavor is hereafter extended towards broader-band prediction, aiming at exploiting broad-band synthetics in further SSI studies. The jump from 5 to 30 Hz is performed by applying the ANN2BB procedure [23]. ANN2BB represents a novel strategy to generate broad-band earthquake ground motions from the results of 3-D physics-based numerical simulations (PBS). Physics-based simulated ground motions embody a rigorous seismic wave propagation model (i.e., including source-, path- and site- effects), which is however reliable only in the LP range (typically for natural periods $T > T^{\star} = 0.75 - 1$ s), owing to the limitations posed both by computational constraints and by insufficient knowledge of the medium at short wavelengths (i.e. the mesh size and the poor description of the fault mechanism and geology). ANN2BB stems from the classical hybridization technique proposed by Graves and Pitarka [5] which consists into enriching the PBS low frequency synthetic wave motion with the classical broad-band wave-forms obtained by stochastic/empirical (STO/EMP) ground motion prediction tools [24]. This achievement is obtained by applying a double filter (high-pass for PBS and low-pass for STO/EMP respectively, see the small axes in FIG. 5a), obtaining hybrid broad-band wave-form (black dashed Sa spectrum in FIG. 5a) that are directly exploitable as spectrum-compatible input motions for seismic design of aboveground structures [25]. Although realistic at the single station, the

STO/EMP prediction fails in rendering the spatial distribution of the short period Intensity Measures (IMs, such as PGA). To cope with these limitation, Paolucci et al. [23] proposed to make use of Artificial Neural Networks (ANN), trained on a set of strong motion records, to predict the response spectral ordinates at short periods. The essence of the procedure (portrayed in FIG. 5b) is (1) to train an ANN on a heterogeneous database of recordings, to then (2) use the trained ANN to estimate the SP response spectral ordinates (red Sa spectrum in FIG. 5b) using as input the long-period ones obtained by the PBS (blue Sa spectrum in FIG. 5b), and, then, to enrich the PBS time-histories at short periods by iteratively scaling their Fourier spectra, with no phase change, until the corresponding response spectrum matches the ANN target spectrum (in small axes in FIG. 5b).

Preliminary tests conducted on such synthetics showed major difficulties and poor effectiveness when trying to match their SP spectrum to ANN prediction, since numerical dispersion polluting PBS time-histories at high-frequencies impoverishes repeatedly the quality of the final broad-band synthetics. Therefore, instead of applying the spectral-scaling technique to PBS synthetics, a classical hybridization mid-step was introduced: the PBS are preliminary hybridized with classical STO/EMP prediction; in a second phase, those broad-band waveforms are spectral-scaled upon the ANN Sa predicted at short-period (applying the corrective factor proposed by [26]). Compared to a standard hybrid approach, ANN2BB yields realistic waveforms, both in time and frequency domains, as well as it renders maps of short-period peak values of ground motion which reproduce more closely the coupling of source-related and site-related features of earthquake ground motion [23]. As a further important asset of the proposed procedure, the approach is suitable to portray in a realistic way the spatial correlation features of the peak values of ground motion, with the possibility to point out possible anisotropies, typically related to the near-source or complex geology conditions.

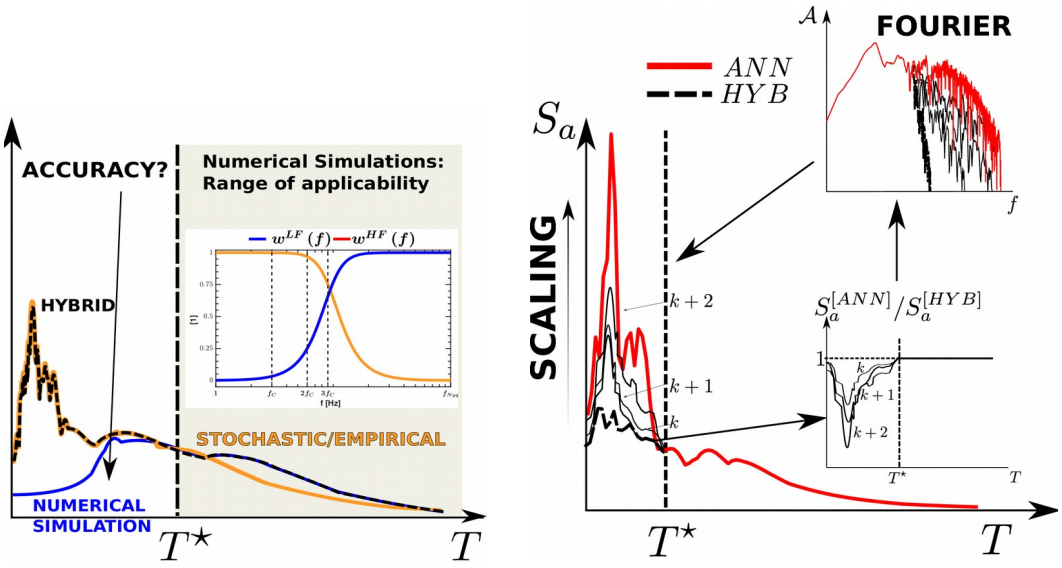

(a) (b)

FIG. 5 (a) Sa response spectra obtained by wave-propagation simulation (PBS, blue), by stochastic/empirical predictive methods (STO/EMP, orange) and by classical hybridization methods of the two (HYB, black dashed), by employing a Butterworth's match filter, composed of a low-cut (LF) and high-cut (HF) filter. (b) Sketch of the Sa spectral matching iterative procedure: the red target spectrum is obtained by ANN prediction and it corresponds to the PBS values at long periods. The SP part is iteratively scaled, starting from the HYB trial, by computing the ratio Sa(ANN) /Sa(HY B) at each iteration and applying it as a corrective scaling factor in the Fourier's domain.

3.2 Broad-band numerical simulation of NCOEQ2007 scenario

Despite the good fit between the SEM3D numerical simulations and the observations, and the high accuracy obtained at 5.0 Hz, it is interesting to apply the ANN2BB technique to the synthetic time-histories obtained. For the sake of simplicity, AS1 was solely considered. An ANN was trained with corner period T*=0.75 s, and applied to the numerical results obtained either with FOLDED geology. FIG. 6a and FIG. 6b portray the site response (in terms of Sa) at the KKNPP Service Hall, for SG4 (G.L.-250 m) and for SG1 (G.L. -2.7 m) respectively. The improved outcome of the broad-band synthetics obtained by ANN2BB confirms somehow the fact that the predictive methodology inherits the information concerning spatial distribution of the earthquake ground motion and it propagates it to shorter periods. This is an interesting phenomenon, since it proves the exceptional capability of neural networks to recognize the input pattern and predict the outcome based on the experience gained during the training phase. Even when SEM3D analyses provided poor fit to the records (probably due to the effect of shallow geotechnical layers, not considered in the numerical analyses), the ANN2BB provides more reasonable spectral ordinates, recommending its utilization to generate realistic broad-band synthetics. It has to be noted that the ANN employed at this stage were trained upon the SIMBAD database [27], containing high-quality recordings observed for earthquakes in a magnitude range M_W 5.0-7.5. Despite the fact that AS1 has a magnitude M_W4.4, the satisfactory results obtained ensure somehow the reliability of the ANN predictive capabilities.

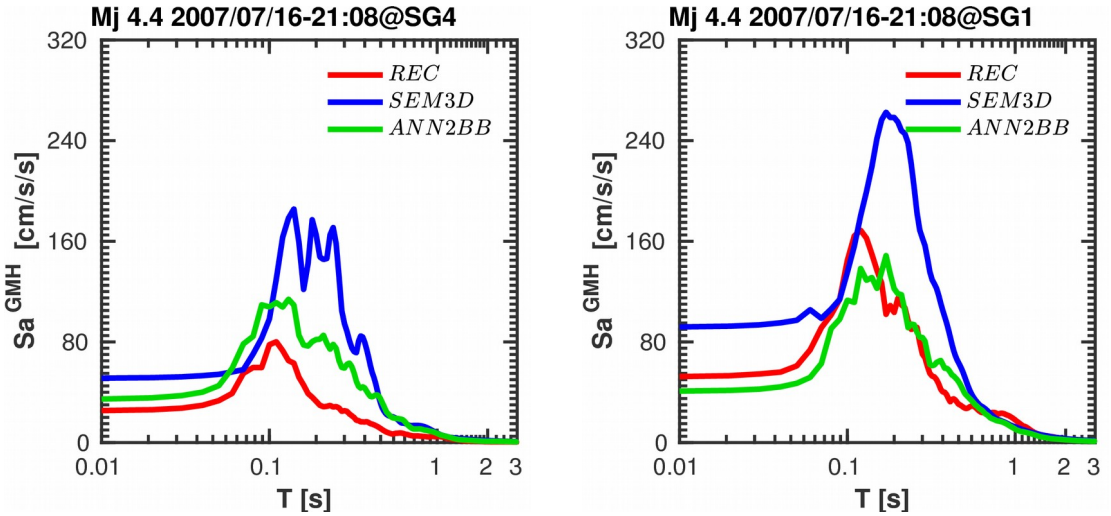

FIG. 6 Sa response spectra (in cm/s^2) after ANN2BB application on the SEM3D analysis performed for AS1, at the Service Hall of the KKNPP site: (a) SG4, G.L. -250 m, (b) SG1, G.L. 0 m respectively. REC (red), SEM3D (blue) and ANN2BB (green) are the recorded, simulated and enriched Sa spectra respectively. Synthetics are filtered at 30.0 Hz.

4. Structural response of a reactor building at KKNPP

4.1 "Feed-forward" weak coupling scheme

The synthetic wave-motion simulated for aftershock AS1 by SEM3D and enriched by ANN2BB was exploited as input motion for a SSI (Soil-Structure Interaction) numerical model (Finite Element Method - Boundary Element Method, FEM-BEM) of the standard reactor building at KKNPP. In this context, a "feed-forward" weak coupling scheme has been conceived (see FIG. 7).

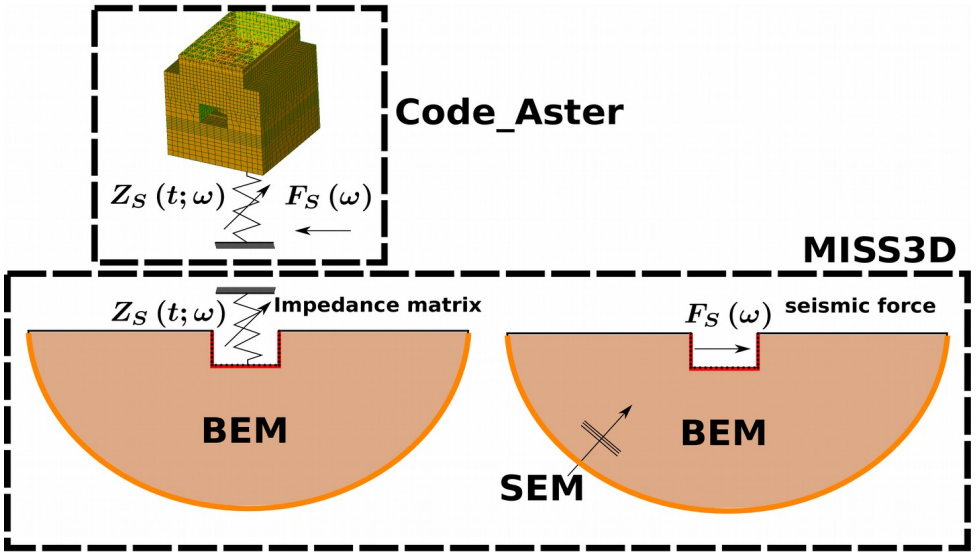

FIG 7. SEM-BEM-FEM coupling scheme to study the KKNPP reactor building. SEM: Spectral Element Method; BEM: Boundary Element Method; FEM: Finite Element Method. Z(t;ω) : non-linear impendance matrix at the soil-structure interface; FS(ω) equivalent seismic force (incident wave motion).

This approach bares upon the domain sub-structuring technique. The computations are carried out by means of coupling between SEM3D+ANN2BB (representing the synthetic broad-band incident wave-field) with MISS3D[1] (BEM), based on the boundary discretization (the soil-structure interface) and it is employed to solve the wave-propagation in a semi-infinite medium (considering the Sommerfeld's conditions) so to compute the impedance matrices and the equivalent seismic forces (in the frequency domain) at the structure basement, and Code_Aster[2] [29] (FEM) to study the dynamic behaviour of bounded domain (i.e. the reactor building) in time, considering geometrical and material non-linearity [30]. In this case, however, the structural transient wave motion was computed in the elastic framework, with the impedance matrices computed (via BEM) for a sub-horizontally layered configuration of homogeneous/isotropic and linear elastic soil domain and the SEM synthetic wave-motion was injected (as wave motion on outcrop bedrock) at the soil-structure interface (embedded footing/foundation slab).

4.2 Seismic response of the KK reactor building

FIG. 9a and 9b show the structural response obtained by inputting the outcropping broad-band synthetic wave motion obtained with SEM3D and enriched by ANN2BB into the coupled BEM-FEM numerical model of the KKNPP Unit 7.

[1]Boundary Element Method (BEM) developed at Ecole Centrale Paris

[2]Finite Element Method (FEM) code developed at Électricité de France (EDF) - https://www.code-aster.org/V2/spip.php?rubrique2

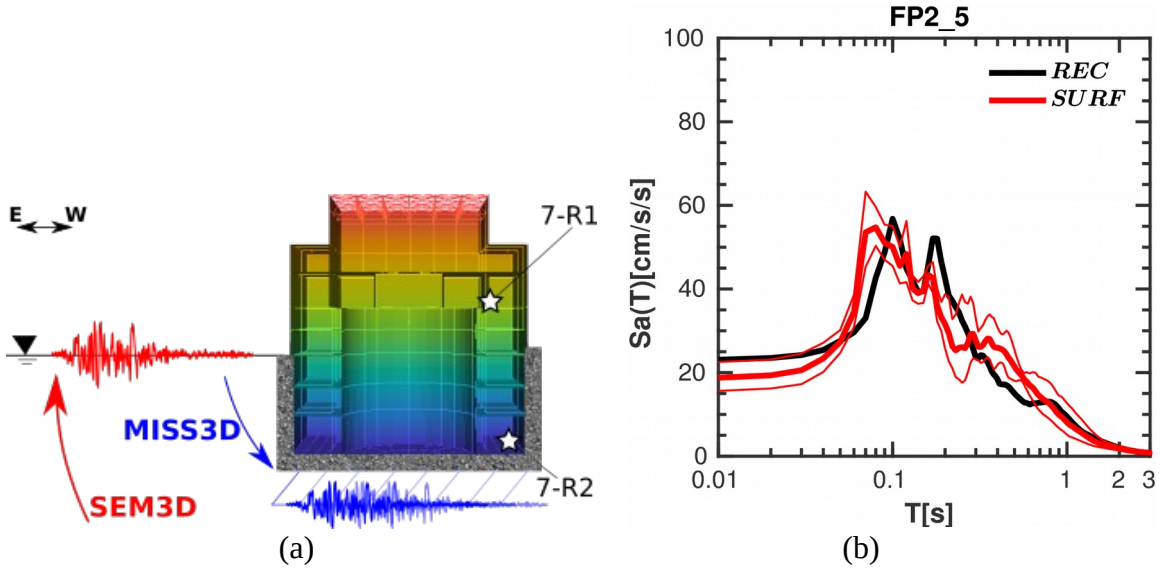

(a) (b)

FIG. 9. (a) Picture of the KKNPP Unit 7 reactor building mesh (Code_Aster). (b) Recorded (black) Sa spectrum (5% damping) at the 5th floor of the reactor building, compared to the synthetic counterpart, obtained by inputting the simulated ground motion at SG1 (surface free-field wave motion, referring at the KKNPP Service Hall). Records and synthetics were both filtered between 0-30 Hz. The Sa response spectra were computed on rotated components of the original EW-NS directions, in a [0-180°] range, with a 10° increment. Thick lines refer to the log-average of the geometric mean on the two horizontal directions, whereas thin lines refer to the log-average +/- standard deviation.

The structural response is presented in terms of Pseudo-Acceleration spectral response Sa (5% damping) at the reactor building basement and at a recording point located at the 5th floor. The inclusion of a complex 3D geology apparently increases the amplitude of the greater Sa peak, without affecting the corresponding natural peak. However, it is of great interest to notice the high uncertainty relatively to the wave planar obliquity: a simple plane rotation of the reference axes (pivoted around the vertical axis) entails slightly different spectra, stressing the analysis of the problem and its sensitivity to the direction considered (inherited by the near-source wave-motion).

5. Conclusions

This study puts in perspective an innovative numerical approach to assess the seismic vulnerability of critical structures. The holistic modeling approach proposes a multi-step simulation of the wave propagation from the source to the structure. The outcropping wave-motion is computed by forward deterministic numerical simulations at regional-scale, in the 0-5 Hz frequency range. The analyses of the Japanese nuclear site of Kashiwazaki-Kariwa (KKNPP), struck by the NCOEQ-2007 event highlighted the great impact of the 3-D geology buried 2 km down deep, but eventually focalizing and selectively amplifying the seismic motion at certain locations within the nuclear site, with the respect to the classical assumption of sub-horizontally layered semi-infinite space. The synthetic time-histories are enriched by applying the ANN2BB procedure, an ANN-based algorithm to predict the short period spectral ordinates and match the input synthetic spectra accordingly. Following this approach, the maximum frequency of the synthetic free-field earthquake ground motion reached f_{max}=30 Hz, compatible with the reference frequency band of common structural vibratory response. The latter was obtained by constructing a FEM model of the nuclear reactor building of the Unit 7 of KKNPP. The input motion produced by SEM regional scale simulation, successively enriched by ANN2BB, was injected as free-field input motion via BEM-FEM coupling. The analysis

unveiled the variability of the numerical prediction of the seismic ground motion, depending on the wave-motion obliquity (typical of near-source condition) and proved the capacity of such numerical methods to reproduce the role played by the complex folded 3-D geology in determining the vulnerability of strategical structures. The weak coupling solution was adopted in the framework of the engineering design standards, neglecting in this study the non-linear SSI (obtained, for via strong coupling scheme in space and time, or by Laplace-Time method [30]).

The case-study presented in this paper proves that the modeling strategy adopted is really appealing for the structural design of critical structures, such as nuclear power plants. However, it is strongly dependent on the degree and detail of knowledge available for the site of interest. In this paper, the effect of the realistic source characteristics were neglected, although the influence of complex ruptures paths on extended fault planes undoubtedly play a crucial role on the structural response. This entails the need to extend the present study to the uncertainty quantification of the source mechanisms. To this end, the scientific work-flow outlined herein is prone to perform this task. Moreover, from a structural design perspective (hazard and vulnerability), the modeling strategy fosters the investigation of seismic contexts characterized by poor observational databases, such as the moderately seismic scenario of metropolitan France, where multiple nuclear installations are present.

Further investigations are however necessary, which will likely be performed by verification and validation benchmarks, so to outline in detail the improvements and the practical performances of the proposed strategy compared to others, as well as possible shortcomings [31]. In the nuclear engineering and industrial contexts, this task is mandatory for a rigorous quality control of the complex toolchain adopted for the design and vulnerability assessment of such critical structures.

6. Acknowledgements

This work, within the SINAPS@ project, benefited from French state funding managed by the National Research Agency under program RNSR Future Investments bearing reference No. ANR-11-RSNR-0022-04. The research reported in this paper has been supported in part by the SEISM Paris Saclay Research Institute.

REFERENCES

[1] Berge-Thierry, C.; Svay, A.; Laurendeau, A.; Chartier, T.; Perron, V.; Guyonnet-Benaize, C.; Kishta, E.; Cottereau, R.; Lopez-Caballero, F.; Hollender, F.; Richard, B.; Ragueneau, F.; Voldoire, F.; Banci, F.; Zentner, I.; Moussallam, N.; Lancieri, M.; Bard, P.-Y.; Grange, S.; Erlicher, S.; Kotronis, P.; Maoult, A. L.; Nicolas, M.; Régnier, J.; Bonilla, F. & Theodoulidis, N. Toward an integrated seismic risk assessment for nuclear safety improving current French methodologies through the SINAPS@ research project Nuclear Engineering and Design, 2017, 323, 185 - 201

[2] De Martin, F. (2011). Verification of a Spectral-Element Method Code for the Southern California Earthquake Center LOH.3 Viscoelastic Case. Bulletin of the Seismological Society of America, 101(6):2855–2865.

[3] Paolucci, R., Mazzieri, I., and Smerzini, C. (2015). Anatomy of strong ground motion: near-source records and 3D physics-based numerical simulations of the Mw 6.0 May 29 2012 Po Plain earthquake, Italy. Geophysical Journal International, 203:2001–2020.

[4] Vazquez, M.; Houzeaux, G.; Koric, S.; Artigues, A.; Aguado-Sierra, J.; Aris, R.; Mira, D.; Calmet, H.; Cucchietti, F.; Owen, H.; Taha, A. & Cela, J. M. Alya (2014). Towards Exascale for Engineering Simulation Codes. International Supercomputing Conference 2014, eprint arXiv:1404.4881

[5] Graves, R. W. & Pitarka, A. (2004) Broadband time history simulation using a hybrid approach. 13th World Conference on Earthquake Engineering, Vancouver, B.C., Canada.

[6] Pavlenko, O. V. and Irikura, K. (2012). Nonlinear Soil Behavior at the Kashiwazaki-Kariwa Nuclear Power Plant During the Niigata Chuetsu-Oki Earthquake (July, 16, 2007). Pure and Applied Geophysics, 169(10):1777–1800.

[7] Gatti, F.; Lopez-Caballero, F.; Paolucci, R. and Clouteau, D. (2017) Near-source effects and non-linear site response at Kashiwazaki-Kariwa Nuclear Power Plant, in the 2007 Chuetsu-Oki earthquake: evidence from surface and downhole records and 1D numerical simulations. Bulletin of Earthquake Engineering. Published online. Doi: 10.1007/s10518-017-0255-y

[8] Watanabe, T., Moroi, T., Nagano, M., Tokumitsu, R., Kikuchi, M., and Nishimura, I. (2009). Analysis of the strong motion records obtained from the 2007 Niigataken Chuetsu-Oki earthquake and determination of the design basis ground motions at the Kashiwazaki Kariwa Nuclear Power Plant. Part 2. Difference of site amplification based on the 2D FEM analysis of the folded structure. Technical report.

[9] Uetake, T., Nishimura, I., and Mizutani, H. (2008). Characteristics of Strong Motion Records In Kashiwazaki-Kariwa Nuclear Power Station during the Niigataken Chuetsu-Oki Earthquake in 2007. In 14th WCEE.

[10] Tsuda, K., Hayakawa, T., Uetake, T., Hikima, K., Tokimitsu, R., Nagumo, H., and Shiba, Y. (2011). Modeling 3D Velocity Structure in the Fault Region of the 2007 Niigataken Chuetu-Oki Earthquake with Folding Structure. In 4th IASPEI/IAEE International Symposium-Effects of Surface Geology on Seismic Motion, pages 1–11.

[11] Shinohara, M.; Kanazawa, T.; Yamada, T.; Nakahigashi, K.; Sakai, S.; Hino, R.; Murai, Y.; Yamazaki, A.; Obana, K.; Ito, Y. & others Precise aftershock distribution of the 2007 Chuetsu-Oki Earthquake obtained by using an ocean bottom seismometer network Earth, planets and space, Springer, 2008, 60, 1121-1126

[12] Hijikata, K., Nishimura, I.and Mizutani, H., Tokumitsu, R., Mashimo, M., and Tanaka, S. (2010). Ground motion characteristics of 2007 Niigata-ken Chuetsu-Oki earthquake. Journal of Structural and Construction Engineering, 75(653):1279–1288.

[13] Tokumitsu, R.; Kikuchi, M.; Nishimura, I.; Shiba, Y. & Tanaka, S. Analysis of the strong motion records obtained from the 2007 Niigataken Chuetsu-Oki earthquake and determination of the design basis ground motions at the Kashiwazaki Kariwa Nuclear Power Plant. Part 1. Outline of the strong motion records and estimation of factors in large amplification 2009

[14] Kobayashi, I.; Tateishi, M.; Yoshimura, T.; Ueda, T. & Kato, T. Geology of the Kashiwazaki District Geological Survey Japan (GSJ), 1995

[15] Gürpinar, A., Serva, L., Livio, F., and Rizzo, P. C. (2017). Earthquake-induced crustal deformation and consequences for fault displacement hazard analysis of nuclear power plants. Nuclear Engineering and Design, 311:69 – 85.

[16] Aochi, H.; Ducellier, A.; Dupros, F.; Delatre, M.; Ulrich, T.; de Martin, F. & Yoshimi, M. Finite difference simulations of seismic wave propagation for the 2007 Mw 6.6 Niigata-ken Chuetsu-Oki earthquake: Validity of models and reliable input ground motion in the near field Pure and Applied Geophysics, hal-00980238, Springer Verlag (Germany), 2013, 170, 43-64

[17] Gatti, F.; Lopez-Caballero, F.; Clouteau, D. & Paolucci, R. (2018). On the effect of the 3-D regional geology on the seismic design of critical structures: the case of the Kashiwazaki-Kariwa Nuclear Power Plant Geophysics Journal International, 2017. https://doi.org/10.1093/gji/ggy027

[18] Cupillard, P., Delavaud, E., Burgos, G., Festa, G., Vilotte, J.-P., Capdeville, Y., and Montagner, J.-P. (2012). RegSEM: a versatile code based on the spectral element method to compute seismic wave propagation at the regional scale. Geophysical Journal International, 188(3):1203–1220.

[19] Festa, G. and Vilotte, J.-P. (2005). The Newmark scheme as velocity-stress time-staggering: an efficient PML implementation for spectral element simulations of elastodynamics. Geophysical Journal International, 161(3):789–812.

[20] Seriani, G. (1998). 3-D large-scale wave propagation modeling by spectral element method on Cray T3E multiprocessor. Computer Methods in Applied Mechanics and Engineering, 164(1):235–247.

[21] de Abreu Corrêa, L.; Camata, J. J.; de Carvalho Paludo, L.; Aubry, L.; Cottereau, R. & Coutinho, A. L. G. A. (2017) Wave propagation in highly heterogeneous media: scalability of the mesh and random properties generator. Submitted for publication in Computers & Geosciences.

[22] Hayakawa, T., Tsuda, K., Uetake, T., Hikima, K., Tokumitsu, R., and Nagumo, H. (2011). Modeling 3D velocity structure in the fault region of the 2007 Niigataken Chuetu-oki Earthquake-Incorporating the 3D fold geological structure beneath the Kashiwazaki-Kariwa nuclear power plant. In Japan Geoscience Union meeting, number SSS023, page 14.

[23] R. Paolucci, F. Gatti, M. Infantino, A. G. Ozcebe, C. Smerzini, M. Stupazzini (2018). Broad-band ground motions from 3D physics-based numerical simulations using Artificial Neural Networks, Bulletin of the Seismological Society of America. Accepted for publication.

[24] Motazedian, D. & Atkinson, G. M. (2005). Stochastic finite-fault modeling based on a dynamic corner frequency. Bulletin of the Seismological Society of America, 95, 995-1010.

[25] C. Smerzini, M. Villani (2012). Broadband Numerical Simulations in Complex Near-Field Geological Configurations: The Case of the 2009 Mw 6.3 L'Aquila Earthquake, Bulletin of the Seismological Society of America 102 (6) 2436–2451. doi:10.1785/0120120002.

[26] A. Shahbazian, S. Pezeshk (2010). Improved Velocity and Displacement Time Histories in Frequency Domain Spectral-Matching Procedures, Bulletin of the Seismological Society of America 100 (6). doi:10.1785/0120090163.

[27] C. Smerzini, C. Galasso, I. Iervolino, R. Paolucci (2014). Ground motion record selection based on broadband spectral compatibility, Earthquake Spectra 30 (4) 1427–1448.

[28] IAEA-TECDOC-1722 (2013). Review of Seismic Evaluation Methodologies for Nuclear Power Plants Based on a Benchmark Exercise. Wien, 2013.

[29] Code_Aster (2001). General public licensed structural mechanics finite element software, included in the Salomé-Méca simulation platform. Website http://www.code-aster.org.

[30] A. Nieto-Ferro, D. Clouteau, N. Greffet, and G. Devésa (2012). On a hybrid Laplace-time domain approach to dynamic interaction problems. European Journal of Computational Mechanics, 21:3–6

[31] Ivo Babuska, J. Tinsley Oden (2004). Verification and validation in computational engineering and science: basic concepts. Comput. Methods Appl. Mech. Engrg. 193, 4057–4066